

## Supporting information

### **Unveiling the critical role of W doping in enhancing oxygen reduction activity of SrCo<sub>0.7</sub>Fe<sub>0.3</sub>O<sub>3-δ</sub> cathode for intermediate temperature SOFCs**

Qian Wang<sup>a,b</sup>, Guanghu He<sup>a,\*</sup>, Xinkun Zhou<sup>a,c</sup>, Wenyuan Liang<sup>a</sup>, Xiuling Wang<sup>a</sup>, Lei Chu<sup>b</sup>, Minghua Huang<sup>b,\*</sup>, Heqing Jiang<sup>a,c,\*</sup>

a State Key Laboratory of Photoelectric Conversion and Utilization of Solar Energy, Qingdao New Energy Shandong Laboratory, Qingdao Institute of Bioenergy and Bioprocess Technology, Chinese Academy of Sciences, Qingdao, China

b School of Materials Science and Engineering Ocean University of China, Qingdao, China

c University of Chinese Academy of Sciences, Beijing 100049, China

Corresponding authors:

[hegh@qibebt.ac.cn](mailto:hegh@qibebt.ac.cn)

[huangminghua@ouc.edu.cn](mailto:huangminghua@ouc.edu.cn)

[jianghq@qibebt.ac.cn](mailto:jianghq@qibebt.ac.cn)

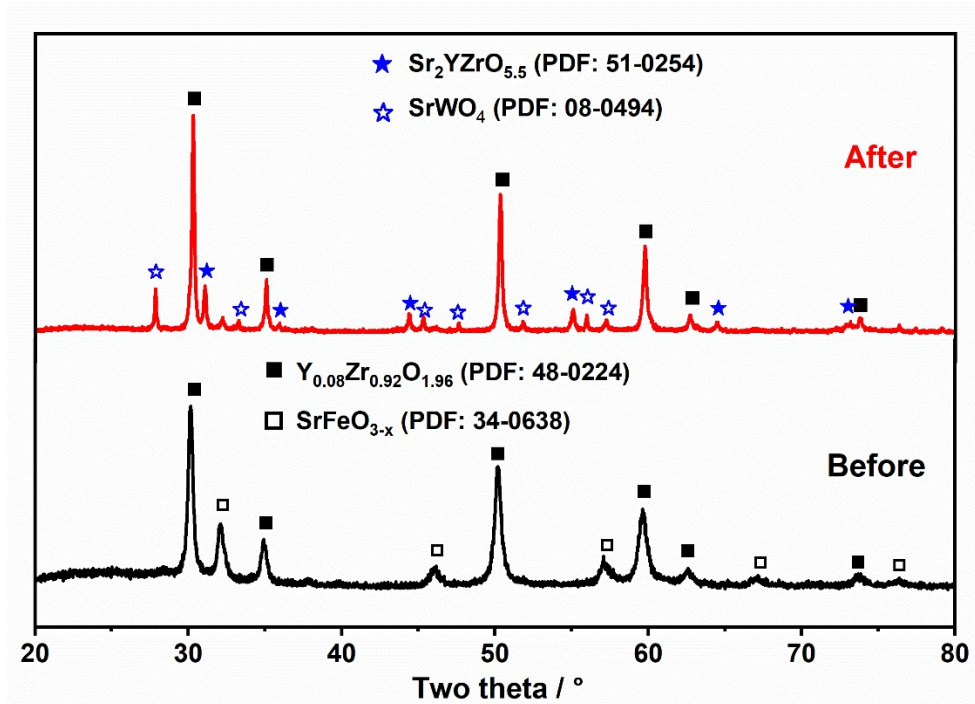


**Figure S1:** XRD patterns of SCFW-0.1 and YSZ powders before and after calcination at 1000 °C for 10h

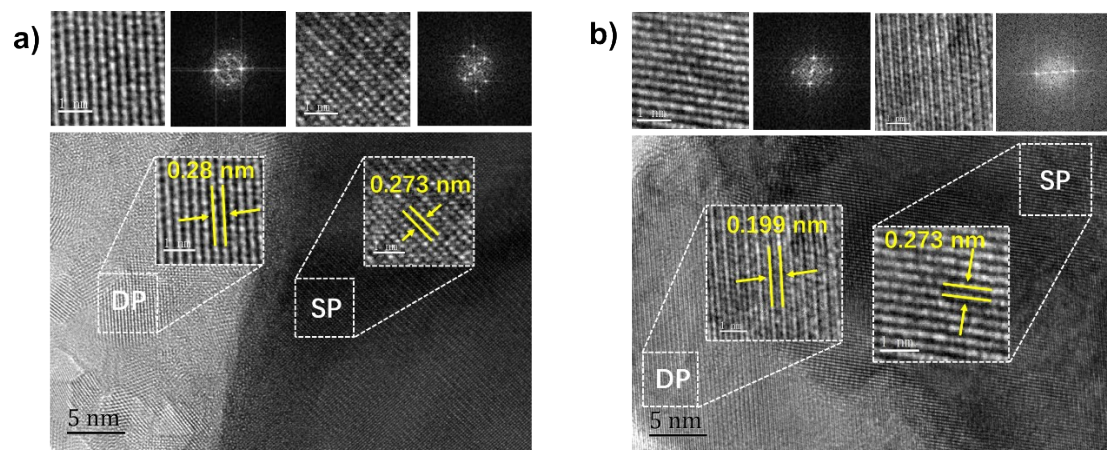


**Figure S2.** HRTEM images of a) SCFW-0.1 and b) SCFW-0.15 oxide.

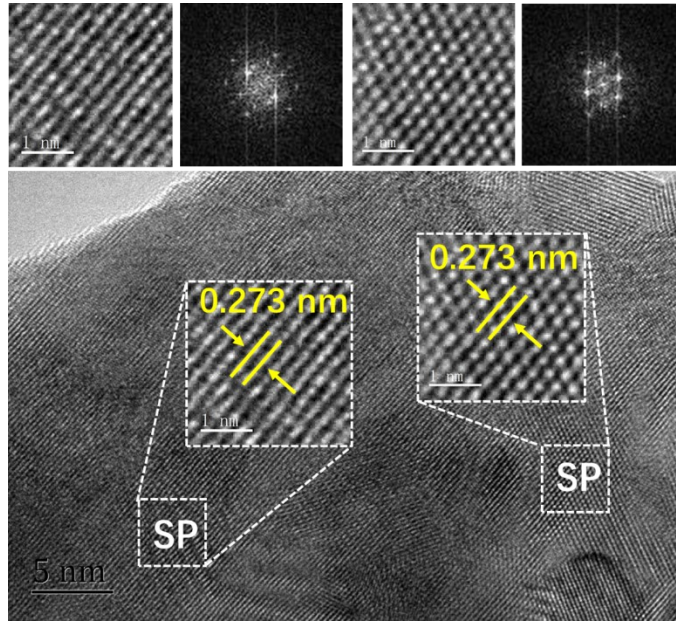


**Figure S3.** HRTEM images of SCF oxide.

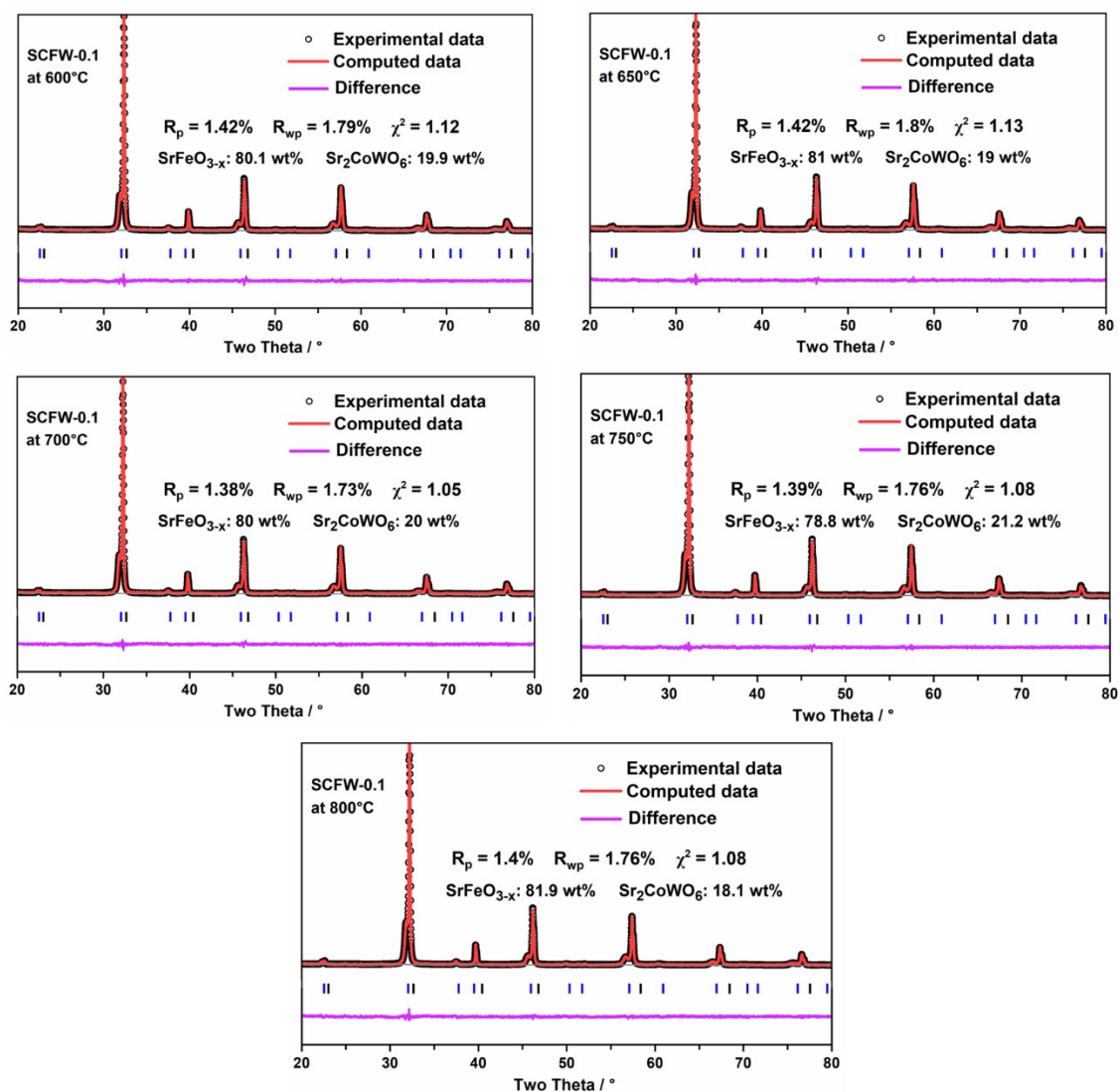


**Figure S4.** Refined XRD patterns of SCFW-0.1 oxide at 600 – 800 °C.

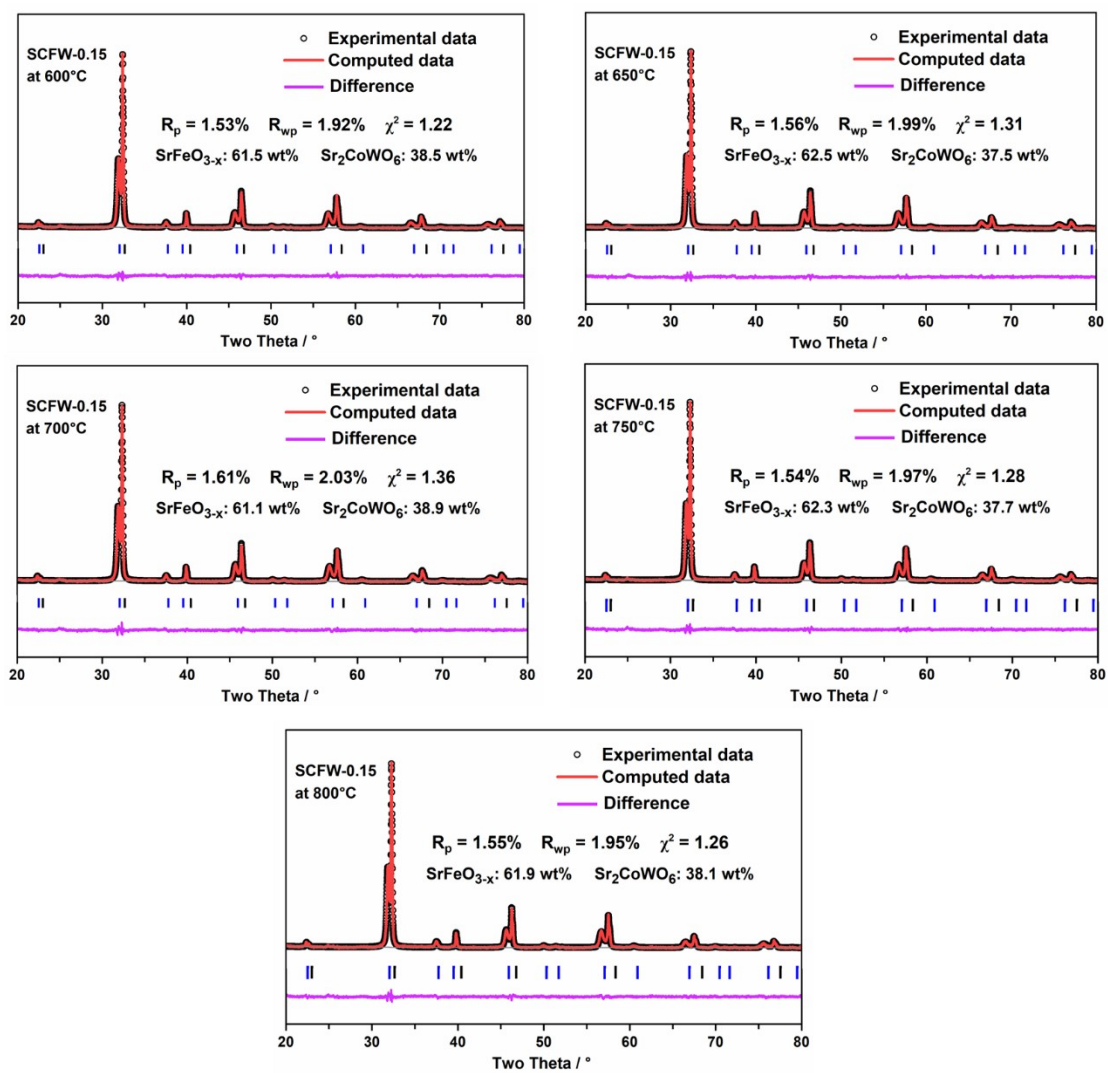


**Figure S5.** Refined XRD patterns of SCFW-0.15 oxide at 600 – 800 °C.

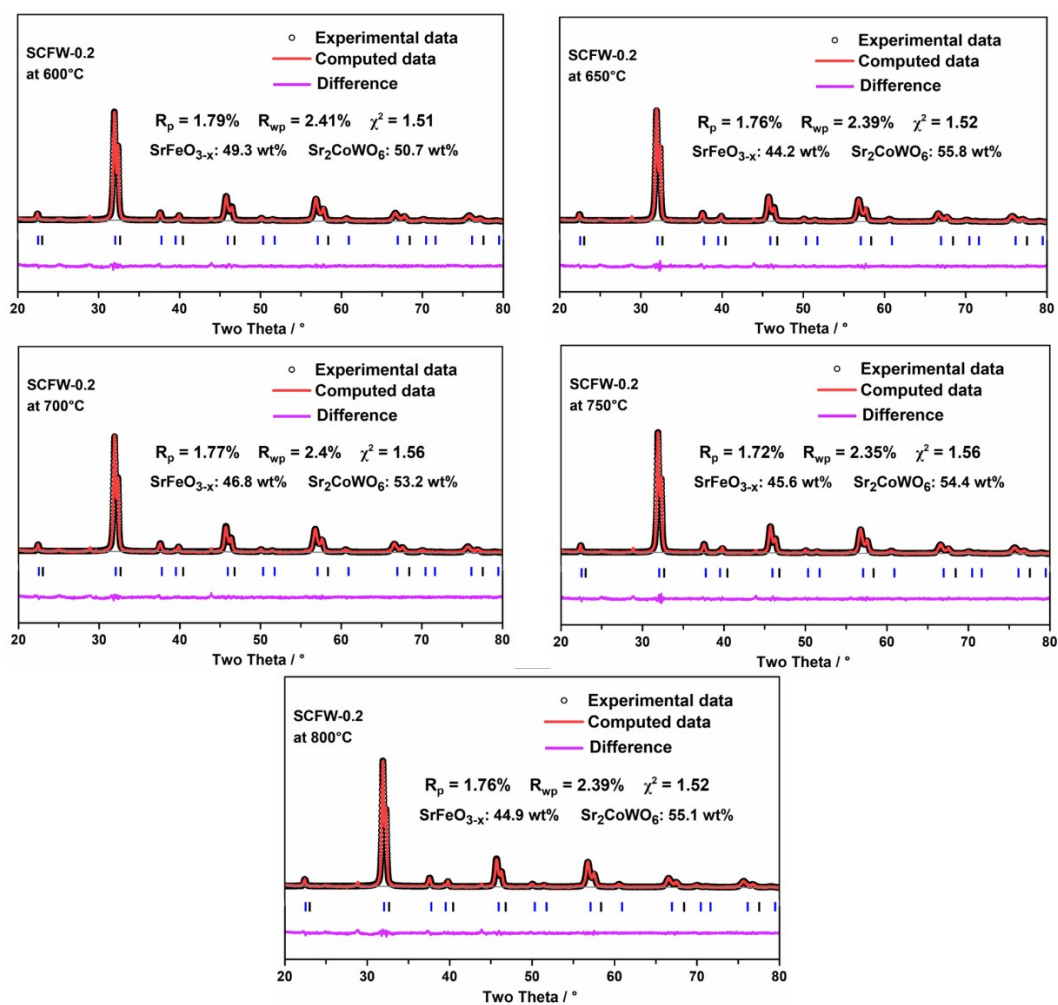


**Figure S6.** Refined XRD patterns of SCFW-0.2 oxide at 600 – 800 °C.

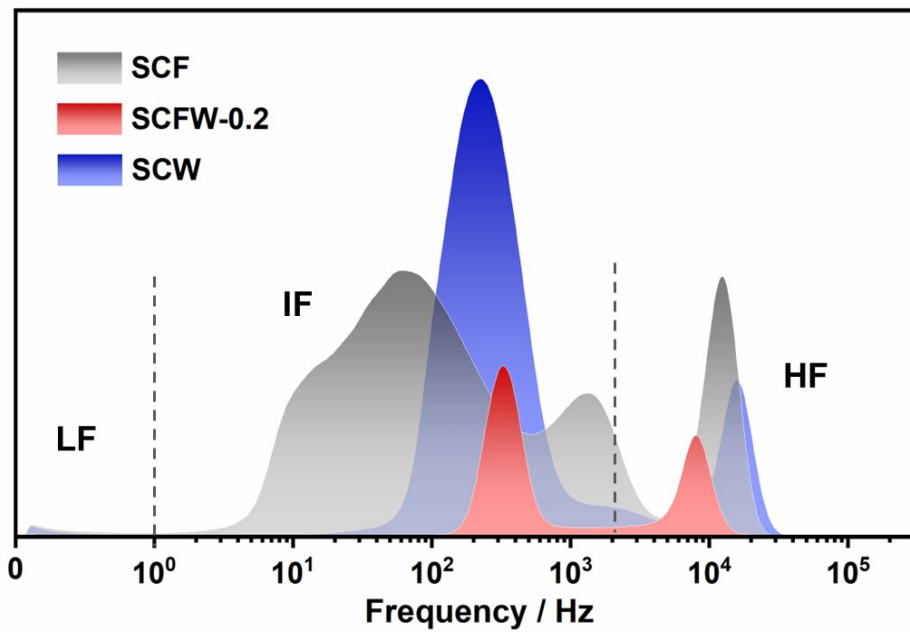


**Figure S7.** Distribution of relaxation time (DRT) analysis of EIS data for SCF, SCFW-0.2 and SCW oxides

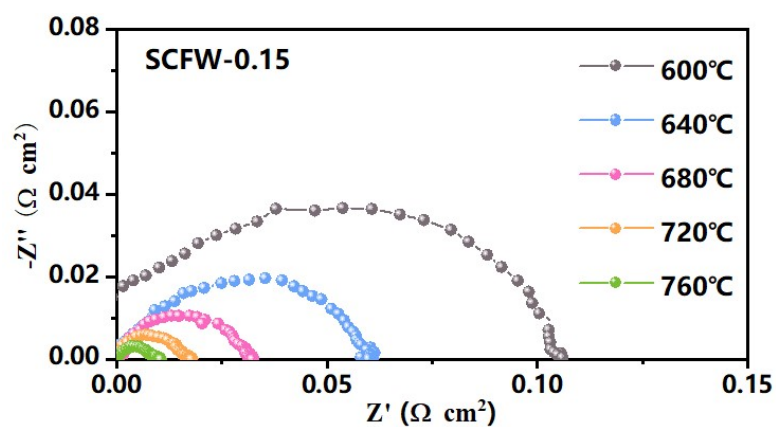
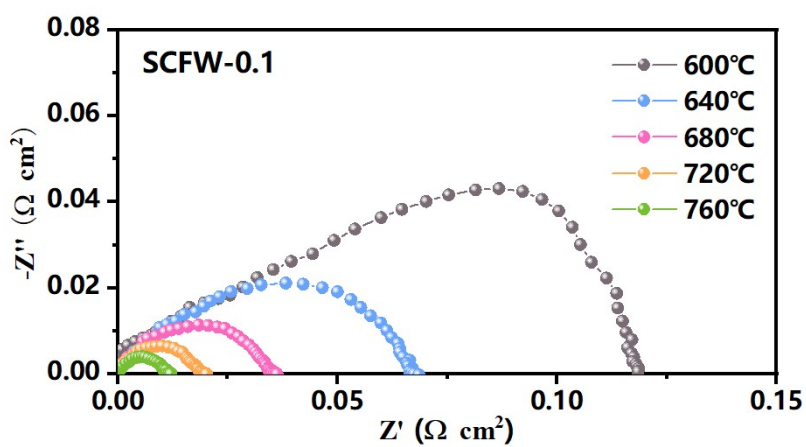


**Figure S8.** EIS curves of  $\text{SrCo}_{0.7}\text{Fe}_{0.3-x}\text{W}_x\text{O}_{3-\delta}$  ( $x=0, 0.1, 0.15, 0.2$  and  $0.3$ ) electrode at different temperatures

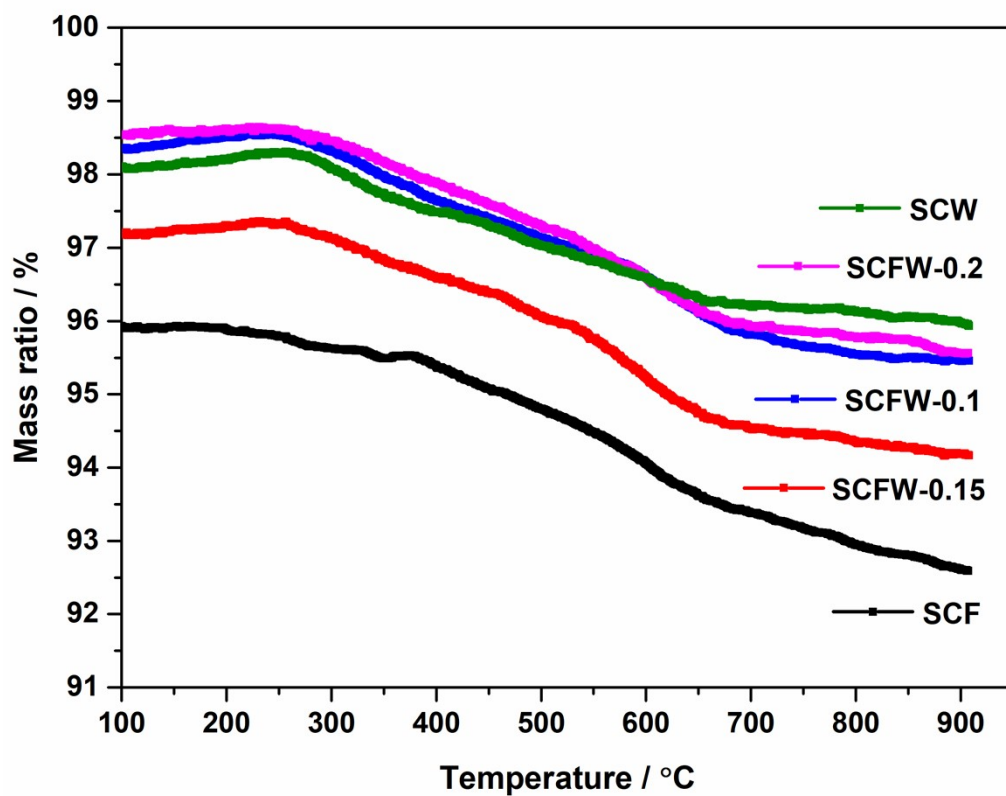
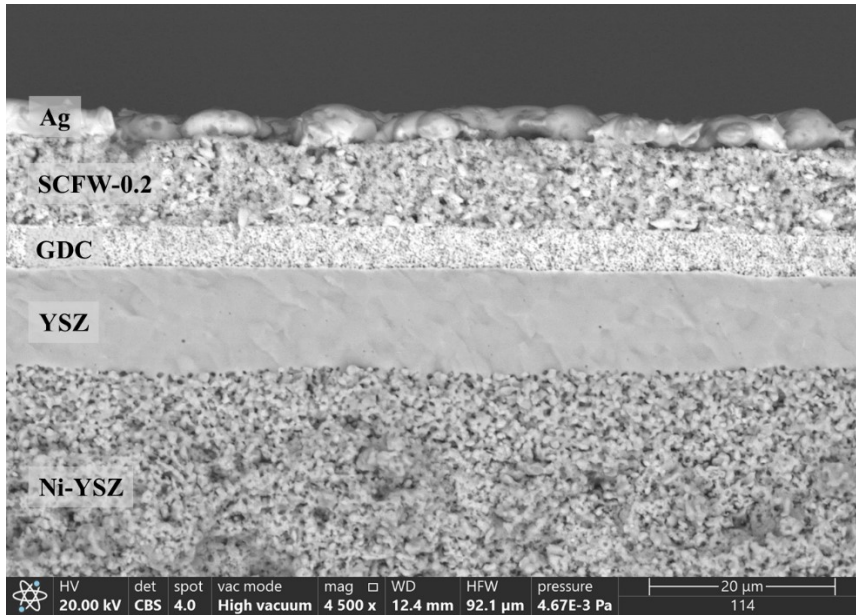
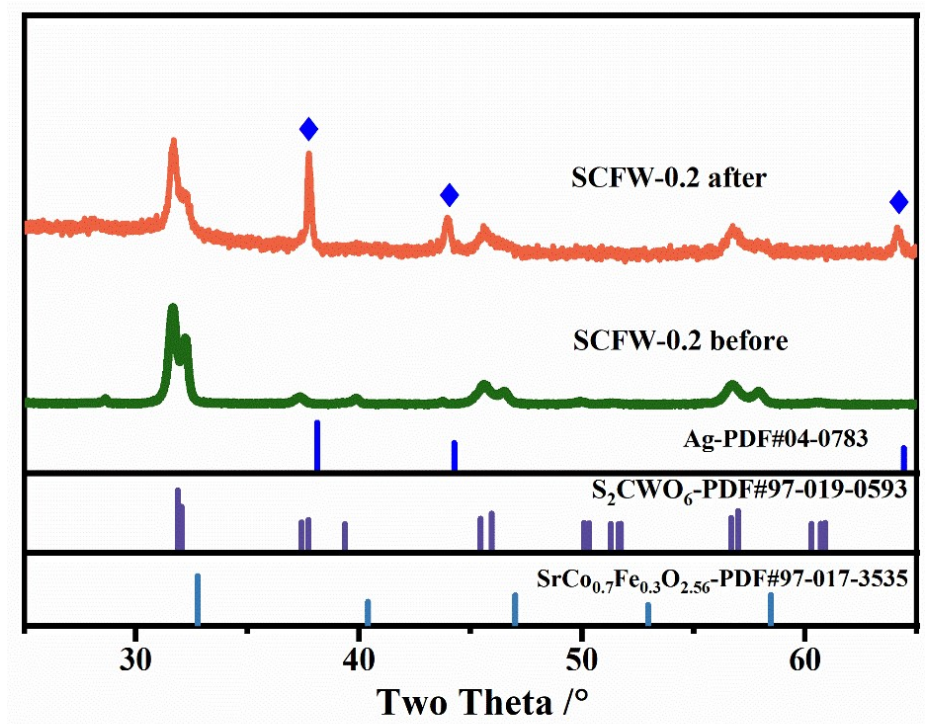


Figure S9. TGA curves of the SCFW oxides.



**Figure S10.** SEM image of the cross-section of the spent cell after 30-h stability test.



**Figure S11.** XRD patterns on the SCFW-0.2 cathode of the spent cell after 30-h stability test.

**Table S1:** The peak power density (PPD) of SCFW-0.2-based SOFC compared with typical perovskite-based SOFC reported in previous literature

Cathode	Electrolyte	Anode	Temp./ °C	PPD / mW cm <sup>2</sup>	Ref.
$(\text{Ba}_{0.5}\text{Sr}_{0.5})_{0.75}\text{Pr}_{0.25}\text{Co}_{0.575}\text{Fe}_{0.3}\text{W}_{0.125}\text{O}_{3-\delta}$	LSGM	LDC/Ni-GDC	650	430	1
$\text{SmBa}_{0.7}\text{Sr}_{0.3}\text{Co}_2\text{O}_{6-\delta}$	SDC	Ni-SDC	700	210	2
$\text{SmBa}_{0.5}\text{Sr}_{0.5}\text{Fe}_2\text{O}_{5+\delta}$	LSGM	SDC/NiCu-SDC	650	180	3
$\text{LaBa}_{0.5}\text{Sr}_{0.5}\text{Fe}_2\text{O}_{6-\delta}$	SDC	Ni-SDC	650	150	4
$\text{Sr}_2\text{Fe}_{1.8}\text{W}_{0.2}\text{O}_{6-\delta}$ -GDC	LSGM	$\text{Sr}_2\text{Fe}_{1.6}\text{W}_{0.4}\text{O}_{6-\delta}$ -GDC	650	150	5
$\text{LaBaFe}_{1.925}\text{Nb}_{0.075}\text{O}_{6-\delta}$	SDC	Ni-SDC	650	255	6
$\text{SrCo}_{0.7}\text{Nb}_{0.1}\text{Ni}_{0.2}\text{O}_{3-\delta}$	GDC/YSZ	Ni-YSZ	650	305	7
$\text{CoFe}_2\text{O}_4$	GDC/YSZ	Ni-YSZ	650	160	8
$\text{SrCo}_{0.7}\text{Fe}_{0.1}\text{W}_{0.2}\text{O}_{3-\delta}$	GDC/YSZ	Ni-YSZ	650	285	This work

LSGM:  $\text{La}_{0.9}\text{Sr}_{0.1}\text{Ga}_{0.8}\text{Mg}_{0.2}\text{O}_{3-\delta}$ ; YSZ:  $(\text{Y}_2\text{O}_3)_{0.08}(\text{ZrO}_2)_{0.92}$ ; GDC:  $\text{Ce}_{0.9}\text{Gd}_{0.1}\text{O}_{2-\delta}$ ; LDC:  $\text{Ce}_{0.9}\text{La}_{0.1}\text{O}_{2-\delta}$ ; SDC:  $\text{Ce}_{0.8}\text{Sm}_{0.2}\text{O}_{2-\delta}$

## Reference

1. Z. Du, L. Shen, Y. Gong, M. Zhang, J. Zhang, J. Feng, K. Li, K. Świerczek, H. Zhao, Self-Assembled Perovskite Nanocomposite With Beneficial Lattice Tensile Strain as High Active and Durable Cathode for Low Temperature Solid Oxide Fuel Cell, *Advanced Functional Materials*, 2024, **34**, 2310790.
2. A. Subardi, C.-C. Chen, M.-H. Cheng, W.-K. Chang, Y.-P. Fu, Electrical, thermal and electrochemical properties of  $\text{SmBa}_{1-x}\text{Sr}_x\text{Co}_2\text{O}_{5+\delta}$  cathode materials for intermediate-temperature solid oxide fuel cells, *Electrochimica Acta*, 2016, **204**, 118-127.
3. D. Guo, A. Li, C. Lu, D. Qiu, B. Niu, B. Wang, High activity and stability of cobalt-free  $\text{SmBa}_{0.5}\text{Sr}_{0.5}\text{Fe}_2\text{O}_{5+\delta}$  perovskite oxide as cathode material for solid oxide fuel cells, *Ceramics International*, 2023, **49**, 34277-34290.
4. H. Li Z. Lü, A highly stable cobalt-free  $\text{LaBa}_{0.5}\text{Sr}_{0.5}\text{Fe}_2\text{O}_{6-\delta}$  oxide as a high performance cathode material for solid oxide fuel cells, *International Journal of Hydrogen Energy*, 2020, **45**, 19831-19839.
5. K. Zheng, J. Lach, P. Czaja, M. Gogacz, P. Czach, A. Brzoza-Kos, P. Winiarz, J. Luo, Designing high-performance quasi-symmetrical solid oxide cells with a facile chemical modification strategy for  $\text{Sr}_2\text{Fe}_{2-x}\text{W}_x\text{O}_{6-\delta}$  ferrites electrodes with in situ exsolution of nanoparticles, *Journal of Power Sources*, 2023, **587**, 233707.
6. H. Li, B. Wei, C. Su, C. Wang, Z. Lü, Novel cobalt-free layered perovskite  $\text{LaBaFe}_{2-x}\text{Nb}_x\text{O}_{6-\delta}$  ( $x=0-0.1$ ) as cathode for solid oxide fuel cells, *Journal of Power Sources*, 2020, **453**, 227875.
7. Y. Lu, L. Ding, M. Li, J. Li, X. Wang, X. Ding, High-performance and  $\text{CO}_2$ -resistant cathode toward electrocatalytic oxygen reduction for solid oxide fuel cells: Doped ceria and  $\text{SrCo}_{0.7}\text{Nb}_{0.1}\text{Ni}_{0.2}\text{O}_{3-\delta}$  composite, *Electrochimica Acta*, 2021, **398**, 139323.
8. Z. Chen, B. Ma, C. Dang, J. Che, L. Cheng, Y. Zhou, A novel strategy of entropy engineering at the A-site in spinel oxides for developing high-performance SOFC cathodes, *Journal of Materials Chemistry A*, 2024, **12**, 24997-25010.